Accepted Manuscript

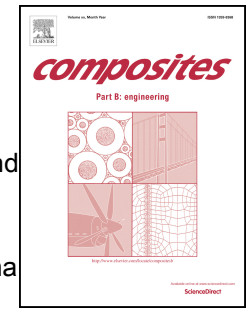

Influence of temperature on the curing of an epoxy adhesive and its influence on bond behaviour of NSM-CFRP systems

Andrea Benedetti, Pedro Fernandes, José L. Granja, José Sena-Cruz, Miguel Azenha

PII: S1359-8368(15)00718-0

DOI: 10.1016/j.compositesb.2015.11.034

Reference: JCOMB 3914

To appear in: *Composites Part B*

Received Date: 1 September 2015

Revised Date: 10 November 2015

Accepted Date: 24 November 2015

Please cite this article as: Benedetti A, Fernandes P, Granja JL, Sena-Cruz J, Azenha M, Influence of temperature on the curing of an epoxy adhesive and its influence on bond behaviour of NSM-CFRP systems, *Composites Part B* (2016), doi: 10.1016/j.compositesb.2015.11.034.

Influence of temperature on the curing of an epoxy adhesive and its influence on bond behaviour of NSM-CFRP systems

Andrea Benedetti[a], Pedro Fernandes[a], José L. Granja[a], José Sena-Cruz[a1], Miguel Azenha[a]

[a] ISISE – Institute for Sustainability and Innovation in Structural Engineering
University of Minho, School of Engineering
Department of Civil Engineering
Campus de Azurém
4800-058 Guimarães
Portugal
Tel: +351 253 510 200; Fax: +351 253 510 217

ABSTRACT

In NSM-CFRP installations, the mechanical behaviour of the strengthening system is strongly influenced by the epoxy adhesive, particularly at early ages. In the present work, the influence of temperature on the curing process of the epoxy was investigated. Three distinct temperatures were studied: 20, 30 and 40 °C. The elastic modulus of the adhesive was monitored through EMM-ARM (Elasticity Modulus Monitoring through Ambient Response Method). Direct pull-out tests with concrete specimens strengthened with NSM CFRP strips were carried out at the same three distinct temperatures to compare the evolution of bond performance with the E-modulus of epoxy since early ages. The results showed that increasing the curing temperature significantly accelerated both the curing process of the epoxy adhesive and the evolution of bond performance. The EMM-ARM technique has revealed its ability in clearly identifying the hardening kinetics of epoxy adhesives, allowing also thermal activation analysis. Finally, existing models for predicting temperature-

[1] Corresponding author: jsena@civil.uminho.pt

dependent mechanical properties were extended to also describe the bond behaviour of NSM-CFRP applications.

KEYWORDS

A. Carbon fibre

A. Theromosetting resin

B. Cure behaviour

D. Non-destructive testing

Near-surface mounted reinforcement

1 INTRODUCTION

The potential of near-surface mounted (NSM) technique using carbon fibre reinforced polymers (CFRP) for strengthening reinforced concrete (RC) structures has been shown in many studies and practical applications [1-5]. Compared to externally bonded reinforcement (EBR), the NSM system presents considerable advantages, such as: larger bond surface induces better anchorage capacity [6]; no preparation work is needed other than grooving; the FRP reinforcement, due to the cover of the surrounding concrete, has an improved protection against environmental effects, such as freeze/thaw cycles, elevated temperatures, fire, and vandalism [7, 8]; less prone to premature debonding due to the larger bonded area and the confinement effect of the grooves, allowing a more efficient use of the reinforcement material. Although a large number of experimental investigations has been carried out on the structural behaviour of NSM FRP strengthened RC structures [3, 4], the effect of the curing conditions on the development of the bond performance is one of the less investigated issues.

It is largely acknowledged that the bond performance of NSM-FRP systems is mainly governed by the mechanical properties of the groove filler [4, 9]. The most employed groove fillers in NSM-FRP systems are two-component epoxy resin-based adhesives [3, 4]. The chemical reactions that occur during the curing period are known to be exothermic and transform the two liquid components of the adhesive to a highly cross-linked space framework by means of polymerization [10]. The parameter that represents the sensitivity of the reaction rate to temperature is the activation energy. This term is defined as the thermal energy required to start the chemical reaction [11] and has to be experimentally determined.

As the polymerization reactions proceed, the material gradually transforms into a rigid solid glass with relevant mechanical properties. Previous investigations indicate that the evolution of the tensile properties (both strength and stiffness) of structural epoxy adhesives strongly depend on the curing temperature [12-15]. Lower curing temperatures considerably decelerate the process and consequently the rate of development of mechanical properties [12-15]. However, the works mentioned above were focused mainly on the adhesive. Only a few investigations were found to be aimed at describing the evolution of the interface behaviour between FRP and concrete (and not only the adhesive) under various distinct curing conditions. Dutta and Mosallam [16] studied the strengths of various adhesive

bonds between FRP and concrete under different curing temperatures and durations by means of a field bond strength measuring system. Czaderski et al. [17] carried out pull-off bond tests on externally bonded CFRP strips glued on concrete at various curing conditions.

Both cited works reached similar conclusions: the time development of strength of an adhesive bond is entirely dependent on curing time and temperature. As both time and temperature increase, the epoxy bond strength increases. Although all experimental observations pointed out the influence of the curing conditions on the development of the mechanical parameters, no formulations have been proposed so far for expressing the relationship between the bond performance at a certain instant in time and the curing condition. In this context, quantifying the effect of curing temperature and age on the development of mechanical properties of structural epoxy resins could significantly improve the quality of the preparation and installation procedures for the strengthening applications.

To bridge this gap, the present research focused on two different types of tests, carried out at three distinct temperatures: 20, 30 and 40 °C. On one hand, EMM-ARM (Elasticity Modulus Measurement through Ambient Response Method) tests were performed on samples of epoxy resin cured at the mentioned temperatures with the objective of describing the evolution of the adhesive stiffness since early ages. The EMM-ARM is a variant of classic resonant frequency methods which allows continuous E-modulus measurements, and was already used for concrete [18], cement pastes, mortars [19], and cement-stabilized soils [20]. After the encouraging results obtained in the first applications of EMM-ARM to epoxy adhesives [21, 22], the present work extends the capability of the methodology to thermal activation testing. Concomitantly, direct pull-out tests were carried out on CFRP strips embedded in concrete blocks and cured at different temperatures, for investigation of how the concrete/adhesive/CFRP bond system is influenced by the curing conditions. A comparison between the evolution of epoxy E-modulus and the maximum pull-out force was performed, evaluating the possibility of a correlation between these two entities. Finally, different existing analytical models were extended for describing the development of the temperature-depended mechanical properties of both the adhesive and the CFRP-to-concrete interface.

2 EXPERIMENTAL PROGRAM

In order to characterize the influence of temperature on the curing process of the epoxy adhesive and its impact on the bond behaviour of NSM-FRP strips, three testing temperatures were considered: 20, 30, and 40 °C. The experimental program, globally presented in Table 1, can be subdivided into the following groups of tests:

(i) EMM-ARM tests on adhesive samples to assess the evolution of the adhesive elastic modulus of the epoxy at different curing temperatures;

(ii) direct pull-out tests on concrete cubic specimens strengthened with CFRP laminate strips, aimed at describing the development of the interface behaviour under variable curing conditions;

(iii) tensile tests performed according to EN ISO 527-2:2012 [23], in order to evaluate the E-modulus value of the hardened epoxy.

A specific denomination was devised for the test specimens, each one being labelled as Xn_Y_Z, where X is the test type (EMM – EMM-ARM test, DPT – direct pull-out test, TT – monotonic tensile test), n is the specimen number within the series, Y is the testing time (in hours or days), and Z corresponds to the test temperature. It is noted that EMM-ARM testing provides continuous results, thus the Y parameter is omitted in the labelling of EMM-ARM test specimens.

A single batch of adhesive mixture (with a volume of ~0.9 litres) was made for all the specimens of each curing temperature, in order to avoid the variability that normally exists between different batches [21]. Moreover, it should be noted that the mixing procedures took place in laboratory environment (with temperature of 20±1 ºC) and all the tests were performed at the same respective curing temperature.

The whole mixing procedure lasted about 4 min and the instant t = 0 was defined as the moment when the epoxy components started to be mixed.

2.1 Materials

Four concrete cylindrical cores with a diameter of 100 mm and a height of 200 mm were used to obtain the compressive strength and the elastic modulus of concrete used in the pull-out specimens, in

accordance to EN 12390-3:2009 [24] and LNEC E397-1993:1993 [25], respectively. An average compressive strength, f_{cm}, of 42.35 MPa, with a coefficient of variation CoV of 5.22%, and an average Young's modulus, E_{cm}, of 38.25 GPa (CoV=8.38%) were obtained at the age of the experimental program (approximately three years after concrete casting). The CFRP strips and the epoxy resin were provided by S&P® Clever Reinforcement. The CFRP strip was the '*CFK 150/2000*', with a nominal thickness of 1.4 mm and a width of 10.0 mm. This laminate is composed of unidirectional fibres in a vinylester matrix and presents a smooth surface. From six uniaxial tensile tests carried out according to ISO 527-5:2009 [26] recommendations, the following properties were obtained: Young's modulus equal to 169.5 GPa (CoV=2.5%), tensile strength equal to 2650 MPa (CoV=1.8%), and ultimate strain equal to 1.6% (CoV=1.8%).

All experimental tests were performed with a commercially available epoxy adhesive termed '*S&P Resin 220*'. This two-component epoxy resin-based adhesive is employed for structural bonding between FRP composite and concrete or steel and is composed of two parts (Part A = resin and part B = hardener). According to the material safety data sheets [27, 28], the resin contains Bisphenol A and neopentyl glycol diglycidyl ether, while the hardener is composed of poly(oxypropylene)diamine, piperazine, 3,6-diazaoctanethylenediamin and triethylenetetramine. Components A and B are mixed at a ratio of 4:1 by weight. According to the manufacturer's product guide specification [29], the modulus of elasticity of the adhesive after 3 days of curing at 20 °C, is larger than 7.10 GPa and the bond strength on concrete is 3 MPa.

2.2 EMM-ARM tests

The EMM-ARM is a variant of the traditional resonance frequency methods that allows the measuring of the material E-modulus since mixing and was already adapted for the study of epoxy adhesives by Granja et al. [21]. This method is based on the identification of the first resonance frequency of a cantilever composite beam filled with the material to be tested. The beam is composed by a 330 mm acrylic tube with external and internal diameters of 20 mm and 16 mm, respectively (see Figure 1). In one of the extremities, a custom made clamping device is attached to the composite beam, in order to ensure the structural system, which is a cantilever with a span of 250 mm.

In order to identify the natural frequency of the beam, a lightweight accelerometer (mass: 5.8 g; sensitivity: 100 mV/g; frequency range: 0.5 to 10000 Hz) is attached to the free end of the cantilever beam that is solely excited by the ambient excitations (e.g., people walking nearby; room ventilation; vibrations produced by mechanical equipment). However, in order to increase the intensity of the ambient noise, a fan is placed in the vicinity of the beam. Based on the vertical accelerations measured, and by means of the Welch procedure [30] (using sub-sets of data with 4096 points (NFFT), Hanning windows with 50% overlap) and a peak picking method [31], the resonance frequency is identified through the peak with highest intensity in the power spectrum density. The measured accelerations were acquired in a 24-bit data logger (NI-USB-9233) with a frequency of 500 Hz, and divided into sets of 5 minutes every 10 minutes. The monitoring procedures started immediately after the correct placement of all components, which occurred within ~20 min after mixing the epoxy adhesive. After the modal identification of the first flexural resonance frequency, the rigidity of the composite beam can be analytically correlated to its frequency through the dynamic equations of the cantilevered structural system. The whole set of equations used for the characterization of E-modulus is explained in [19]. The final solution is the differential equation shown below:

$$a^3\left[\cosh(a\cdot L)\cdot\cos(a\cdot L)+1\right]+\frac{w^2\cdot m_p}{EI}\left[\cos(a\cdot L)\cdot\sinh(a\cdot L)-\cosh(a\cdot L)\cdot\sin(a\cdot L)\right]=0 \quad (1)$$

where $a=\sqrt[4]{w^2\times\bar{m}/EI}$, EI corresponds to the distributed flexural stiffness of the composite beam, $\bar{m}$ is the uniformly distributed mass per unit length, m_p is the concentrated mass at the free extremity of the cantilever, L is the span of the cantilever, f is the first flexural resonant frequency, and $w=2\pi f$ is the corresponding angular frequency.

Therefore, for each identified resonant frequency, f, it is possible to obtain the corresponding EI of the composite beam, and since the acrylic E-modulus E_a is known, the Young modulus of the tested epoxy adhesive E_e can be estimated through the equation:

$$EI=E_a\frac{\pi(\varphi_e^4-\varphi_i^4)}{64}+E_e\frac{\pi\varphi_i^4}{64} \quad (2)$$

where φ_e and φ_i are the outer and inner diameters, respectively. In this way, it is possible to relate the first natural frequency of the composite beam with the elastic modulus of the tested epoxy during the testing time. As in this work it was intended to perform EMM-ARM measurements at different temperatures, the E-Modulus of the acrylic mould was accessed before each test at the testing temperature through modal identification of the empty acrylic tubes [32], following the same protocol presented before. In order to check the method's ability to obtain results with good repeatability, two tests were performed simultaneously.

2.3 Pull-out tests

As previously referred, in order to assess the evolution of bond behaviour of concrete elements strengthened with NSM-CFRP systems during the hardening of the epoxy adhesive under different curing temperatures, thirty monotonic direct pull-out tests were carried out for the specific ages (see Table 1). Figure 2 shows the specimen geometry and the test configuration adopted for the monotonic direct pull-out tests. The specimen consisted of a concrete cubic block of 200 mm edge, into which a NSM-CFRP laminate strip with 1.4 mm thickness and 10 mm width was inserted. The strengthening detail and a cross-section of the groove are presented in Figure 2a. The groove was performed with a fix saw cut machine. A constant bond length, L_b of 60 mm, filled with the epoxy adhesive was adopted. The justification for such fixed value of the bond length can be found elsewhere [33]. To avoid premature splitting in the concrete ahead the loaded end, the bond length started 100 mm far from the top of the block. To assure negligible vertical displacement at the top of the concrete specimen during pull-out test, a steel plate with 20 mm thickness was applied at the top of the concrete block. This plate was fixed to the support base through four M10 steel threaded rods. A torque of 30 N×m was applied, inducing an initial compression to concrete of about 2.0 MPa. The pull-out tests were performed on a closed steel frame equipped with a servo-controlled equipment. As previously mentioned, the testing temperature was the same as that of the corresponding curing. For this purpose, a custom-made temperature chamber was manufactured with Expanded Polystyrene plates (see Figure 2b). A heater was placed inside a climatic chamber and an automatic system (thermostat equipped

with a platinum resistor thermometer (PT100) sensor) was used to control the imposed temperature. Additionally, a thermocouple type k was placed near to the bond region.

A LVDT (range ±2.5 mm with a linearity error of ±0.05% F.S.) was used to measure the slip at the loaded end, s_l. The applied force, F, was registered by a load cell of 200 kN of capacity (with a linearity error less than ±0.05% F.S.) placed between the load actuator and the grip. The tests were performed under displacement control at a rate of 2 μm/s, assessed by another LVDT placed between the actuator and the grip. Before strengthening, several measurements were carried out for each specimen to assess the actual geometry of the grooves, using a digital calliper with an accuracy of ±0.01 mm (see Table 2).

The strengthening of the specimens was carried out when the grooves were completely dry and clean. The strengthening was performed at laboratory environment (T=21±2 ºC) for all the studied temperatures. Afterwards, the specimens were put into the previously described temperature chamber (which occurred within ~20 min since the epoxy components started to be mixed) and were kept under controlled temperature until the age of testing. It is important to remark that, before the strengthening procedure, the adhesive epoxy was kept in the climatic chamber at T=20±1ºC and RH=60±5%. Detailed description about the specimen preparation and strengthening procedure can be found elsewhere [33].

3 RESULTS AND DISCUSSION

3.1 Epoxy E-modulus

The development of the epoxy E-moduli obtained through EMM-ARM at the three curing temperatures under test (20, 30 and 40 ºC) are presented in Figure 3a. The results of tensile tests are shown in Figure 4 and also added to the Figure 3a. The modulus of elasticity was calculated from tensile test results based on the highest slope of the stress-strain curve, in accordance with the work of Moussa et al. [34]. Observation of EMM-ARM results in Figure 3a allows verifying that the E-modulus curves corresponding to the same temperature have very good coherence with each other, with absolute stiffness differences under 3.0% at all instants (~0.27 GPa at the age of 144 hours at 20 ºC), demonstrating adequate repeatability of EMM-ARM. Furthermore, there is a good agreement

between the E-Modulus estimated through the EMM-ARM and the tensile tests, with stiffness differences under 3.2% (~0.31 GPa for the 40 ºC test).

In addition, the results show that the reaction rates intensify with the increase of the curing temperature, since it can be observed that, for example, the elastic modulus of 4 GPa is achieved at approximately 10.7 hours at 20 ºC as opposed to the approximately 6.2 and 5.5 hours at 30 and 40ºC, respectively. These variations also occur in the duration of the dormant period. With the increase in the curing temperature the duration of the dormant period becomes shorter, as can be observed in the Figure 3b. At the reference temperature (20 ºC) the setting time (herein defined as the time when the E-Modulus reached 0.25 GPa) was 4.5±0.2 hours, as opposed to the shorter 2.6 hours observed in the test at 40 ºC.

It should also be noted that the E-Modulus of the epoxy at 144 hours increased slightly with the increase of the curing temperature, reaching final values of 8.9, 9.3 and 9.5 for the tests at 20, 30 and 40 ºC, respectively, in accordance with observations made by several previous works on epoxy adhesives [34-36]. This phenomenon can be mainly attributed to a higher cross-link density formation of the epoxy resin cured at higher temperatures. Typically, higher temperatures produce a more complete reaction with a greater degree of cross-linking than lower temperatures, providing sufficient kinetic energy to quickly initiate chemical reactions at even the most hindered locations [36]. It is well-known that increasing the cross-link density leads to improvements in the mechanical properties of epoxy polymers [37-39].

3.2 Pull-out force

The main results of the monotonic pull-out tests are summarized in Table 3. In order to assess the evolution of bond performance, the following parameters were analysed: the maximum pull-out force, $F_{l,max}$; the slip at the loaded end at $F_{l,max}$, $s_{l,max}$; the average bond strength at the CFRP-epoxy interface, τ_{max} that is evaluated by the expression $F_{l,max}/(P_f\, L_b)$, where P_f is the perimeter of the CFRP cross-section in contact with the adhesive and L_b is the bond length. Table 3 also provides information about the failure mode of the tested specimens, with the following codes: D=debonding at CFRP-epoxy interface; FE=cohesive shear failure in epoxy; CC=concrete cracking; SE=splitting of epoxy.

The relationship between the pull-out force and slip at loaded end ($F_l - s_l$) for all tested specimens at three different temperatures (20, 30 and 40 ºC) of curing are presented in Figures 5a, b and c. It is possible to observe the increase on bond stiffness along the curing of epoxy adhesive. This evolution process seems to be totally governed by the state of hardening of the adhesive. The process of hardening depends on the curing temperature, as can be seen in the Figure 5. At 20 °C the pull-out force remains approximately zero at the age of 6 hours, since the epoxy has not yet begun to harden. On the other hand, at the same testing age, the maximum pull-out forces of 5.36 kN and 10.46 kN are achieved at 30 and 40 ºC, respectively. According to the obtained results for 20 and 30 ºC, the authors decided to perform a pull-out test at 40 ºC for the age of 4 hours. As can be seen in Figure 5c, at the age of 4 hours, the epoxy has already begun to harden, with a maximum pull-out force of 2.6 kN.

For the three analysed temperatures, the bond stiffness had a significant increase from 6 to 24 hours, showed by the sharp slope difference of the curves obtained by the tests performed between 6 and 24 hours. However, for 40 ºC, at 12 hours the $F_l - s_l$ response exhibit the bond-slip behaviour similar for ages higher than 24 hours, when the epoxy has achieved a significant maturity level. In general, after the first 24 hours the bond stiffness did not show any significant variation. In terms of average maximum pull-out force considering the specimens tested at 72 hours at 30 ºC and 40 ºC the values were very close (27.79±0.03 kN) and were higher (9.2 % on average) than those of 20 ºC, that is consistent with the obtained final values of epoxy E-modulus (see Figure 3a).

Regarding to the failure modes, it is possible to observe that at the early ages until ~12 hours the failure mode tend to be cohesive and occurring in the adhesive by shear failure (FE), as Table 3 shows, confirming the low mechanical properties of the adhesive at the beginning of the curing. This type of failure mode has been also reported and observed by other researchers e.g. [40, 41]. Furthermore, in some specimens, the performed tests also led to cracking of the epoxy cover and fracture in the concrete along inclined planes (at ~72 hours for 20 °C and at 24 and 72 hours for 40 °C).

It is important to underline that for high pull-out forces (~25 kN), for the test temperatures T30 and T40 the failure mode still occurs by shear failure (cohesive in epoxy), when compared to the test temperature T20, where this type of failure mode only happens for low values of pull-out force (~14 kN). These results indicate that the temperature of curing plays a key role on a global behaviour.

For the description of the pull-out test results, a fitting equation based on the one proposed by Silva, Azenha [20] in the context of E-modulus predictions was used. The proposed equation expresses the evolution of pull-out force according to:

$$F(t) = F_{ult} \exp\left[-\frac{1}{2}\left(\frac{\lambda}{t}\right)^{\beta}\right] \quad (3)$$

where F_{ult} is the average of experimental values for the specimens tested from 72 hours; β is the reaction shape parameter and λ is the reaction time parameter. This model was applied in order to use the methods for obtaining the activation energy that will be shown in the next section. Regression analyses were performed to determine these parameters, using experimental values (see Table 4). The best fit was achieved using the method of least squares, in order to maximize the coefficient of determination between the model and the experimental curve. By observing Figure 6 it is possible to verify that the use of Equation (3) allows to obtain a very good estimate of pull-out force evolution ($0.969 \leq R^2 \leq 0.982$), even at the early stages of the curing.

Finally, it should be noted that F_{ult} is variable with temperature. This happens because the failure modes occurred in the pullout tests were governed by the mechanical properties of the adhesive (see Table 3), which are improved by increased curing temperatures (in the range tested here). Similar behaviours have also been observed and reported by previous research works [42]. It is however noted that, according to the literature [43], for the cases where the failure is cohesive within the concrete, the maximum load carrying capacity of NSM-CFRP concrete systems are not affected by the curing temperature (in the range tested here).

3.3 Relationship between pull-out force and E-modulus

With the purpose of evaluating the possibility of a correlation between the interface behaviour of NSM systems and the epoxy stiffness, a comparison between the peak pull-out force and the adhesive E-modulus is carried out for the three studied temperatures, as shown in Figure 7. In order to compare better the results pertaining to different temperatures, all the values were normalized in regard to the measurements obtained at the age of 72 hours. Figure 7a highlights that the peak pull-out force and the

epoxy E-modulus obtained by EMM-ARM exhibit very similar evolution kinetics, thus indicating that the bond performance of NSM CFRP system strongly depends on the stiffness of the adhesive regardless of the curing temperature. The increase on bond stiffness is consistent with the stage at which the rate of thermosetting reactions is higher, although its development was slightly delayed compared to E-modulus development. During the analysis of the results, the authors also analysed the possibility of correlating bond stiffness obtained from the pullout tests and elastic modulus of the epoxy adhesive. However, due to the high dispersion obtained in this correlation along the curing time, the comparison between both parameters was unfeasible, and the authors decided not to include it herein. As opposed, the correlation between elastic modulus and maximum pull-out force is valid taking into account the observed failure modes, which are governed by the mechanical properties of the epoxy adhesive and/or the mechanisms of adhesion between CFRP and epoxy (cohesive in epoxy and debonding at CFRP-epoxy interface). Figure 7b illustrates the relationship between the E-modulus of the epoxy-resin and the maximum pull-out force for the different curing temperatures: the scatter in the measured properties tended to be highest when the slope of the curves in Figure 7a was steepest and then decreased for later ages. The slight difference on the kinetics of the two properties seems to be similar for all temperatures and may be attributed to a delay in the development of the molecular bond quality, which usually has less influence on the stiffness of the epoxy resin than on its strength [12]. Based on this kind of relationship, EMM-ARM can be employed for estimating the maximum pull-out force and the minimum curing time to reach a threshold value of pull-out force. In this manner it is possible to know the time required to put the strengthened structure in service, taking into account the influence of different environmental curing conditions.

4 KINETIC MODELLING

A kinetic analysis is presented in the following paragraphs to describe the experimental results of both the adhesive E-modulus and pull-out force. Two different approaches were considered for the kinetic analysis. The first approach was based on fitting the experimental data to an assumed reaction model, better known as phenomenological model [44]. The data was fitted to a single-step reaction model that yields a single averaged value of the activation energy for the overall cure process. An alternative

approach to the phenomenological model is the model-free isoconversional method [45] , also used in the present work. Without assuming a particular form of the reaction model, this latter method allows evaluating the effective activation energy as a function of the extent of the cure. The activation energy can be considered a time-temperature shift factor and as such it is useful in predicting the time to reach a specific curing degree as a function of temperature. This concept, well-known as time-temperature superposition [46], can be expressed by a relationship which relates the times to reach a certain conversion at two different temperatures (T_{cure} and T_{ref}). Prime [47] proposed the following isoconversion Arrhenius relationship:

$$t_{eq} = \sum_{0}^{t} \exp\left[\frac{E_a}{R}\frac{(T_{cure} - T_{ref})}{T_{ref}T_{cure}}\right] \cdot \Delta t \tag{4}$$

Where t is the instant at which the equivalent age is being computed, t_{eq} is the equivalent age at the reference temperature T_{ref}, T_{cure} is the temperature of cure, E_a is the activation energy, and R is the gas constant (8.314 kJ/mol·K). Therefore, a time-temperature shifting was performed using the activation energy calculated for both phenomenological model and isoconversional method, thus allowing a comparison between the two different methods.

4.1 Autocatalytic model

In the context of curing process of different materials the autocatalytic model has a widespread acceptance and is typically used. The curing reaction can be described by a rate equation given by the following expression [48]:

$$\frac{d\alpha}{dt} = k(T)f(\alpha) \tag{5}$$

where α is the curing degree, $d\alpha/dt$ is the curing rate, T is absolute temperature (in K), $k(T)$ is the rate constant, and $f(\alpha)$ is the function that describes the curing reaction mechanism. Here, the curing degree is quantified as follows:

$$\alpha(t) = \frac{E(t)}{E_{ult}} \tag{6}$$

E(t), E_{ult}: monitored E-modulus of epoxy resin at age *t*, and E-modulus at 144 hours. Based on the EMM-ARM results, a kinetic model of autocatalytic curing reactions was assumed [46], namely:

$$f(\alpha) = \alpha^m (1-\alpha)^n \tag{7}$$

where *m* and *n* are the reaction orders independent of temperature, and α^m represents the catalytic effect. This function exhibits a delayed cure rate peak, which occurs during the curing process, while at the beginning of the reaction (*t* = 0), the term curing rate, *dα/dt*, is zero for all temperatures. The reaction parameters *k*, *m* and *n* were obtained by fitting the isothermal data [49] with the non-linear least square regression method based on the Generalized Reduced Gradient algorithm [50]. The relationship between the curing rate and the curing degree is shown in Figure 8. Experimental results were satisfactorily simulated by the selected autocatalytic model. At 20 °C, the maximum curing rate occurred at a curing degree of approximately 25%, while at higher curing temperatures (30 and 40 °C) the curves exhibited a lightly delayed peak at around 32% curing degree. The kinetic rate constant *k* follows an Arrhenius temperature dependence [51]:

$$k(T) = A \exp\left(-\frac{E_a}{RT}\right) \tag{8}$$

A: proportionality constant; E_a: activation energy of epoxy resin (J/mol); *R*: gas constant (8.314 kJ/mol K). The kinetic rate equation can therefore be rewritten as:

$$\frac{d\alpha}{dt} = f(\alpha) A \exp\left(-\frac{E_a}{RT}\right) \tag{9}$$

By plotting the logarithms of the rate constant *ln(k)* versus *1/T*, it was possible to obtain both the activation energy, E_a, and the natural logarithm of the pre-exponential factor, *ln(A)*, from the slope and the *y* intercept of a linear fit of the results shown in Figure 9a. Their values, together with the reaction parameters, are given in Table 5. The activation energy was determined to be 34.05 kJ/mol. In Figure 9b the curing degree values are plotted as a function of equivalent age. From this figure, a poor quality of the superposition can be visually identified. The fact that the points in Figure 9a are not aligned confirms that the autocatalytic model activation energy concept was not effective for describing the obtained experimental results, since the activation energy depends on the temperature interval. In fact, the obtained value ends up to be an intermediate value.

4.2 Model-free isoconversional method

This method is based on the single-step kinetic equation and is founded on the isoconversional principle, which states that at a constant extent of conversion, the reaction rate is only a function of the temperature [45]. The Arrhenius equation for two different tests can be described by the following expression:

$$\left(\frac{d\alpha}{dt}\right)_i = f(\alpha_i) A \exp\left(-\frac{E_a}{RT_i}\right) \tag{10}$$

where i = 1, 2 represents each of the two tests. By taking the same fixed value of the curing degree ($\alpha_1 = \alpha_2$) and dividing one equation by the other yields:

$$\left(\frac{d\alpha}{dt}\right)_1 = \left(\frac{d\alpha}{dt}\right)_2 \exp\left(-\frac{E_a}{R}\left(\frac{1}{T_1}-\frac{1}{T_2}\right)\right) \tag{11}$$

Thus, for each value of the curing degree α, a corresponding model-free value of the activation energy is obtained:

$$E_a(\alpha) = -\frac{R}{T_1 - T_2} \ln \frac{\left(\frac{d\alpha}{dt}\right)_1}{\left(\frac{d\alpha}{dt}\right)_2} \tag{12}$$

This method allows calculation of the activation energy from two different tests, and does not require any information about the cure mechanism. However, this equation gives no indication about the reaction order and Arrhenius pre-exponential factor. The analysis of experimental results enabled to plot E_a as a function of the curing degree for each couple of EMM-ARM tests (see Figure 10a). Comparing the relationship of the curing degree with the equivalent age for both studied models, it is possible to observe that the isoconversional method leads to better results, i.e. the superposition of the curves for all the tested specimens, as can be seen in Figure 10b.

Taking account of the results obtained for the E-modulus, the same strategy was applied to the pull-out force only by means of the model-free method. Here, the curing degree is quantified as follows:

$$\alpha(t) = \frac{F(t)}{F_{ult}} \tag{13}$$

where $F(t)$ is the pull-out force at age t and F_{ult} is the ultimate pull-out force of the model. The evolution of the activation energy with the curing degree for the pull-out force is plotted in Figure 11a. The evolution of the E_a curves presented similar shape in comparison with EMM-ARM specimens. Despite the similarity of between the activation energy values obtained for the E-modulus and pull-out force evolutions for the temperatures 20-40 ºC (e.g. both around 19.3 kJ/mol at curing degree of 0.5 with difference of 8.8%), there is a significant difference for the temperatures 20-30 ºC the values of the activation energy exhibit a considerable difference (difference of 28.0% for the curing degree of 0.5). This fact indicates that the influence of temperature on the activation energy is different in these two properties. In Figure 11b the pull-out force curves are plotted as a function of equivalent age. It is possible to confirm the capability of the method to predict the activation energy of both epoxy E-modulus and pull-out force as a time-temperature shift factor. Therefore it is possible to predict the time to reach a specific conversion as a function of temperature.

5 CONCLUSIONS

The present paper presented an experimental study for the evaluation of the influence of temperature on the curing process of the structural epoxy and its impact on the bond behaviour of NSM-CFRP strengthening applications. Three distinct temperatures were studied: 20, 30 and 40 °C. The elastic

modulus of the adhesive was continuously monitored through EMM-ARM. Concomitantly, direct pull-out tests were carried out on CFRP strips embedded in concrete blocks and cured at different temperatures, in order to investigate how the bond between concrete and NSM-CFRP is influenced by the curing conditions. A comparison between the evolution of epoxy E-modulus and the maximum pull-out force was performed, evaluating the possibility of a correlation between these two entities. Finally, different existing analytical models were extended for describing the kinetic analysis of both the evolution of E-modulus and the pull-out force. The main conclusions of the study can be summarized as follows:

1. EMM-ARM has confirmed its capability to access the E-modulus of epoxies adhesives with adequate repeatability in accordance to previous works [21, 22], and it further demonstrated capability to perform studies at temperatures up to 40 ºC. The method was also able to assess the increase of the epoxy stiffness with the increase of the curing and testing temperatures.
2. The E-modulus results shows that the reaction rates intensify with the increase of the curing temperature during both the dormant and the hardening periods.
3. The bond behaviour of NSM-CFRP concrete systems is totally governed by the state of hardening of the adhesive. The process of hardening depends on the curing temperature. For the three analysed temperatures, the bond stiffness and maximum pull-out force had a significant increase from 6 to 24 hours. For 40 ºC, after 12 hours of curing the $F_l - s_l$ response exhibits a bond-slip behaviour similar to ages when the epoxy can be considered cured. The increase on bond stiffness and maximum pull-out force are consistent with the stage at which the rate of thermosetting reactions is higher, although its development was slightly delayed compared to E-modulus development. In general, after the first 24 hours the bond stiffness and bond strength did not show any significant variation.
4. In terms of failures modes, the failure mode was cohesive in the adhesive due to the low mechanical properties of the adhesive at the beginning of the curing, and after certain curing degree the failure mode changed from cohesive shear failure in epoxy to debonding at CFRP-epoxy interface. However, the transition point changed with curing temperature, i.e. increasing

the curing temperature, the transition occurs at higher values of pull-out force (e.g. for the test temperatures T20 and T40, the transition point occurs for 14 kN and 23 kN, respectively).

5. The results obtained through EMM-ARM allowed the estimation of activation energy evolution throughout the whole epoxy curing process by application of the model-free isoconversional method. This model has further shown adequate performance to estimate the activation energy of pull-out force as a time-temperature shift factor when compared to the autocatalytic model.
6. Despite the fact that the autocatalytic model has a widespread acceptance, being typically used in similar contexts, for the present case it turned out to perform poorly for describing the obtained experimental results, since the activation energy depends on the curing temperature.
7. The evolution of the activation energy presented similar shape between the E-modulus and pull-out force. Furthermore the activation energy exhibits a significant temperature dependence, i.e. increasing the curing temperature the activation energy increase. This dependency was also different for the two evaluated entities (E-modulus and pull-out force).
8. Despite the present results being credible, contributing for the knowledge in this area, further investigation is required to better understand the influence of curing temperature on evolution kinetic of the mechanical properties of the epoxy adhesive and properties of adhesion between materials, as well as to confirm the observed tendencies.

6 ACKNOWLEDGEMENTS

This work is supported by FEDER funds through the Operational Program for Competitiveness Factors - COMPETE and National Funds through FCT - Portuguese Foundation for Science and Technology under the projects FRPreDur FCOMP-01-0124-FEDER-028865 (FCT no. PTDC/ECM-EST/2424/2012) and VisCoDyn FCOMP-01-0124-FEDER-041751 (FCT no. EXPL/ECM-EST/1323/2013). The authors also like to thank all the companies that have been involved supporting and contributing for the development of this study, mainly: S&P Clever Reinforcement Ibérica Lda., Artecanter - Indústria de Transformação de Granitos, Lda., Vialam – Indústrias Metalúrgicas e

Metalomecânicas, Lda. The second and third authors also acknowledge the grants SFRH/BD/80338/2011 and SFRH/BD/80682/2011, respectively, provided by FCT.

REFERENCES

[1] Rizzo A, De Lorenzis L. Behavior and capacity of RC beams strengthened in shear with NSM FRP reinforcement. Construction and Building Materials. 2009;23(4):1555-67.
[2] Rizkalla S, Hassan T, Hassan N. Design recommendations for the use of FRP for reinforcement and strengthening of concrete structures. Progress in Structural Engineering and Materials. 2003;5(1):16-28.
[3] De Lorenzis L, Teng JG. Near-surface mounted FRP reinforcement: An emerging technique for strengthening structures. Composites Part B: Engineering. 2007;38(2):119-43.
[4] Coelho MRF, Sena-Cruz JM, Neves LAC. A review on the bond behavior of FRP NSM systems in concrete. Construction and Building Materials. 2015(0).
[5] Garzón-Roca J, Sena-Cruz JM, Fernandes P, Xavier J. Effect of wet-dry cycles on the bond behaviour of concrete elements strengthened with NSM CFRP laminate strips. Composite Structures. 2015;132(0):331-40.
[6] Sena-Cruz JM, Barros JAO, Coelho MRF, Silva LFFT. Efficiency of different techniques in flexural strengthening of RC beams under monotonic and fatigue loading. Construction and Building Materials. 2012;29(0):175-82.
[7] Silva P, Fernandes PMG, Sena-Cruz J, Azenha M, Barros JA. Behaviour of concrete elements strengthened with near surface mounted CFRP strips under thermal cycles. CICE 2014. Vancouver, Canada 2014.
[8] Szabó ZK, Balázs GL. Near surface mounted FRP reinforcement for strengthening of concrete structures. Civil Engineering. 2007;51(1):33-8.
[9] Borchert K, Zilch K. Bond behaviour of NSM FRP strips in service. Structural Concrete. 2008;9:127-42.
[10] Gillham JK. Formation and properties of thermosetting and high Tg polymeric materials. Polymer Engineering & Science. 1986;26(20):1429-33.
[11] Sbirrazzuoli N, Vyazovkin S. Learning about epoxy cure mechanisms from isoconversional analysis of DSC data. Thermochimica Acta. 2002;388(1):289-98.
[12] Moussa O, Vassilopoulos AP, de Castro J, Keller T. Early-age tensile properties of structural epoxy adhesives subjected to low-temperature curing. International Journal of Adhesion and Adhesives. 2012;35:9-16.
[13] Dodiuk H, Kenig S. Low temperature curing epoxies for structural repair. Progress in Polymer Science. 1994;19(3):439-67.
[14] Matsui K. Effects of curing conditions and test temperatures on the strength of adhesive-bonded joints. International Journal of Adhesion and Adhesives. 1990;10(4):277-84.
[15] Lapique F, Redford K. Curing effects on viscosity and mechanical properties of a commercial epoxy resin adhesive. International Journal of Adhesion and Adhesives. 2002;22(4):337-46.
[16] Dutta PK, Mosallam A. A rapid field test method to evaluate concrete composite adhesive bonding. International Journal of Materials and Product Technology. 2003;19(1):53-67.
[17] Czaderski C, Martinelli E, Michels J, Motavalli M. Effect of curing conditions on strength development in an epoxy resin for structural strengthening. Composites Part B: Engineering. 2012;43(2):398-410.
[18] Azenha M, Magalhães F, Faria R, Cunha Á. Measurement of concrete E-modulus evolution since casting: A novel method based on ambient vibration. Cement and Concrete Research. 2010;40(7):1096-105.
[19] Azenha M, Faria R, Magalhães F, Ramos L, Cunha Á. Measurement of the E-modulus of cement pastes and mortars since casting, using a vibration based technique. Mater Struct. 2012;45(1-2):81-92.
[20] Silva J, Azenha M, Correia AG, Ferreira C. Continuous stiffness assessment of cement-stabilised soils from early age. Geotechnique. 2013;63(16):1419-32.
[21] Granja JL, Fernandes P, Benedetti A, Azenha M, Sena-Cruz J. Monitoring the early stiffness development in epoxy adhesives for structural strengthening. International Journal of Adhesion and Adhesives. 2015;59:77-85.
[22] Fernandes P, Granja JL, Benedetti A, Sena-Cruz J, Azenha M. Quality control and monitoring of NSM CFRP systems: E-modulus evolution of epoxy adhesive and its relation to the pull-out force. Composites Part B: Engineering. 2015;75:95-103.

[23] ISO. 527-2:2012 Plastics - Determination of tensile properties - Part 2: Test conditions for moulding and extrusion plastics. Genève, Switzerland: International Oganization for Standardization; 2012.
[24] EN. 12390-3 Testing hardened concrete. Compressive strength of test specimens. Part 3: Compressive strength of test specimens. BSI; 2009.
[25] LNEC. E397-1993 Betões – Determinação do modulo de elasticidade em compressão Documentação Normativa Especificação LNEC [In Portuguese]; 1993.
[26] ISO. 527-5:2009 Plastics - Determination of tensile properties - Part 5: Test conditions for unidirectional fibre-reinforced plastic composites. Genève, Switzerland: International Oganization for Standardization; 2009.
[27] S&P. S&P Resin 220 (Comp A), Safety data sheet. 2013. p. 8.
[28] S&P. S&P Resin 220 (Comp B), Safety data sheet. 2011. p. 6.
[29] S&P. S&P Resin 220 epoxy adhesive, Technical Data Sheet. 2013. p. 3.
[30] Welch PD. The use of fast Fourier transform for the estimation of power spectra: A method based on time averaging over short, modified periodograms. Audio and Electroacoustics, IEEE Transactions on. 1967;15(2):70-3.
[31] Oppenheim AV, Schafer RW. Discrete-Time Signal Processing: Prentice Hall Press; 2009.
[32] Granja J, Azenha M, Sousa Cd, Ferreira C. Comparison Between Different Experimental Techniques for Stiffness Monitoring of Cement Pastes. Journal of Advanced Concrete Technology. 2014;12(2):46-61.
[33] Fernandes PMG, Silva PM, Sena-Cruz J. Bond and flexural behavior of concrete elements strengthened with NSM CFRP laminate strips under fatigue loading. Engineering Structures. 2015;84(0):350-61.
[34] Moussa O, Vassilopoulos AP, de Castro J, Keller T. Time–temperature dependence of thermomechanical recovery of cold-curing structural adhesives. International Journal of Adhesion and Adhesives. 2012;35:94-101.
[35] Lionetto F, Maffezzoli A. Monitoring the Cure State of Thermosetting Resins by Ultrasound. Materials. 2013;6(9):3783-804.
[36] Sun L, Pang S-S, Sterling AM, Negulescu II, Stubblefield MA. Thermal analysis of curing process of epoxy prepreg. Journal of Applied Polymer Science. 2002;83(5):1074-83.
[37] Shokuhfar A, Arab B. The effect of cross linking density on the mechanical properties and structure of the epoxy polymers: molecular dynamics simulation. Journal of molecular modeling. 2013;19(9):3719-31.
[38] Ahmad Z, Ansell M, Smedley D. Thermal properties of epoxy-based adhesive reinforced with nano and micro-particles for in-situ timber bonding. Int J Eng Technol. 2010;10(2):32-8.
[39] Sancaktar E, Jozavi H, Klein RM. The Effects of Cure Temperature and Time on the Bulk Tensile Properties of a Structural Adhesive. The Journal of Adhesion. 1983;15(3-4):241-64.
[40] Teng J, De Lorenzis L, Wang B, Li R, Wong T, Lam L. Debonding Failures of RC Beams Strengthened with Near Surface Mounted CFRP Strips. Journal of Composites for Construction. 2006;10(2):92-105.
[41] Blaschko M. Bond behaviour of CFRP strips glued into slits. Sixth International Symposium on FRP Reinforcement for Concrete Structures (FRPRCS-6): World Scientific; 2003. p. 8-10.
[42] Palmieri A, Matthys S, Taerwe L. Influence of High Temperature on Bond between NSM FRP Bars/Strips and Concrete. ACI Special Publication. 2011;275:1-12.
[43] Klamer EL, Hordijk DA, Hermes MC. The influence of temperature on RC beams strengthened with externally bonded CFRP reinforcement. Heron. 2008;53(3):157-85.
[44] Yousefi A, Lafleur P, Gauvin R. Kinetic studies of thermoset cure reactions: a review. Polymer Composites. 1997;18(2):157-68.
[45] Vyazovkin S, Sbirrazzuoli N. Isoconversional kinetic analysis of thermally stimulated processes in polymers. Macromolecular Rapid Communications. 2006;27(18):1515-32.
[46] Bilyeu B, Brostow W, Menard KP. Epoxy thermosets and their applications. III. Kinetic equations and models. J Mater Ed. 2001;23:189-97.
[47] Prime RB. CHAPTER 5 - Thermosets. In: Turi EA, editor. Thermal Characterization of Polymeric Materials: Academic Press; 1981. p. 435-569.

[48] Vyazovkin S. Handbook of thermal analysis and calorimetry: Recent advances, techniques and applications. In: Brown ME, Gallagher PK, editors. Amsterdam: Elsevier; 2011.
[49] Xia L, Zuo L, Zha S, Jiang S, Guan R, Lu D. Kinetic research on low-temperature cure of epoxy adhesive. International Journal of Adhesion and Adhesives. 2014;50(0):255-64.
[50] Abadie J. The GRG Method for Nonlinear Programming. In: Greenberg HJ, editor. Design and implementation of optimization software. Netherlands: Sijthoff & Noordhoff [International Publishers]; 1978. p. 335-63.
[51] Arrhenius S. On the reaction rate of the inversion of non-refined sugar upon souring. Z Phys Chem. 1889;4:226-48.

LIST OF TABLES

Table 1 – Experimental program

Table 2 – Geometry measurements of the grooves (average values)

Table 3 – Pull-out test results.

Table 4 – Regression parameters obtained from model for the evolution of pull-out force

Table 5 – Kinetic parameters obtained from autocatalytic isothermal model

LIST OF FIGURES

Figure 1 – Experimental setup of EMM-ARM tests (exploded view).

Figure 2 – Configuration of direct pull-out tests: (a) cross-section of the specimen; (b) view of the experimental setup.

Figure 3 – (a) Evolution of epoxy E-modulus along curing time; (b) setting time *versus* curing temperature.

Figure 4 – Average stress-strain curves obtained by tensile tests

Figure 5 – Pull-out force *versus* loaded end slip during curing time at different temperatures: (a) 20 °C; (b) 30 °C and (c) 40 °C.

Figure 6 – Pull-out force *versus* curing time at different temperatures.

Figure 7 – (a) Epoxy E-modulus and peak pull-out force along curing time, normalized to 72 hours; (b) Relationship between epoxy E-modulus and pull-out force.

Figure 8 - Curing rate *versus* curing degree: comparison of experimental and autocatalytic model results.

Figure 9 - Autocatalytic model: (a) Arrhenius plot of rate coefficient; (b) Curing degree of epoxy adhesive *versus* equivalent age.

Figure 10 – Model-free method applied to epoxy E-modulus: (a) Activation energy *versus* curing degree; (b) normalized E-modulus of epoxy adhesive *versus* equivalent age (reference: 20 °C).

Figure 11 – Model-free method applied to pull-out force: (a) Activation energy *versus* curing degree for the pull-out force; (b) Pull-out force *versus* equivalent age (reference: 20 °C).

1 Table 1 – Experimental program

Testing method	**Testing Time**	**20 °C**	**30 °C**	**40 °C**
Pull-out	4h	-	-	DPT1_4h_T40
	6h	DPT1_6h_T20	DPT1_6h_T30	DPT2_6h_T40
	8h	-	DPT2_8h_T30	DPT3_8h_T40
	9h	DPT2_9h_T20	-	-
	10h	-	DPT3_10h_T30	DPT4_10h_T40
	11h	DPT3_11h_T20	-	-
	12h	-	DPT4_12h_T30	DPT5_12h_T40
	13h	DPT4_13h_T20	-	-
	24h	DPT5_24h_T20	DPT5_24h_T30	DPT6_24h_T40
		DPT6_24h_T20	DPT6_24h_T30	DPT7_24h_T40
	72h	DPT7_72h_T20	DPT7_72h_T30	DPT8_72h_T40
		DPT8_72h_T20	DPT8_72h_T30	DPT9_72h_T40
	7d	DPT9_7d_T20	DPT9_7d_T30	DPT10_7d_T40
		DPT10_7d_T20	DPT10_7d_T30	-
EMM-ARM	0h-7d	EMM1_T20	EMM1_T30	EMM1_T40
		EMM2_T20	EMM2_T30	-
Tensile test	7d	TT_7d_T20	TT_7d_T30	TT_7d_T40

2

1 Table 2 – Geometry measurements of the grooves (average values)

Curing temperature	Depth [mm]	Width [mm]
DPT_T20	14.13 (2.66%)	5.21 (2.92%)
DPT_T30	15.21 (2.86%)	5.03 (2.17%)
DPT_T40	14.91 (1.48%)	4.94 (3.08%)

2 The values between parentheses are the corresponding coefficients of variation.

1 Table 3 – Pull-out test results.

Curing temperature	**Time**	**Real testing time** [h]	**Denomination**	$F_{l,max}$ [kN]	τ_{max} [MPa]	$s_{l,max}$ [mm]	**Failure mode**
20 °C	6h	5.9	DPT1_6h_T20	0.02	0.01	-	FE
	9h	8.9	DPT2_9h_T20	3.07	2.24	0.97	FE
	12h	11.2	DPT3_11h_T20	9.11	6.66	1.64	FE
		12.8	DPT4_13h_T20	13.63	9.96	1.27	FE
	24h	24.5	DPT5_24h_T20	26.27	19.20	0.64	D
		25.9	DPT6_24h_T20	25.76	18.83	0.55	D
	72h	72.2	DPT7_72h_T20	26.17	19.13	0.72	D
		73.2	DPT8_72h_T20	27.24	19.91	0.68	D+SE+CC
	7d	168.6	DPT9_7d_T20	24.50	17.91	0.49	D
		169.9	DPT10_7d_T20	23.87	17.45	0.56	D
30 °C	6h	6.02	DPT1_6h_T30	5.36	3.92	1.55	FE
	8h	7.98	DPT2_8h_T30	12.73	9.31	1.47	FE+D
	10h	10.0	DPT3_10h_T30	17.98	13.14	1.09	FE+D
	12h	12.0	DPT4_12h_T30	21.38	15.63	0.80	FE
	24h	24.2	DPT5_24h_T30	27.88	20.38	0.71	FE+D
		25.3	DPT6_24h_T30	26.59	19.44	0.75	FE+D
	72h	72.4	DPT7_72h_T30	28.78	21.04	0.89	D
		73.5	DPT8_72h_T30	25.70	18.79	0.72	D
	7d	168.1	DPT9_7d_T30	26.71	19.52	0.72	D
		169.5	DPT10_7d_T30	29.83	21.81	0.84	D
40 °C	4h	4.2	DPT1_4h_T40	2.60	1.90	1.01	FE
	6h	6.1	DPT2_6h_T40	10.46	7.65	1.49	FE
	8h	8.1	DPT3_8h_T40	19.49	14.25	1.12	FE
	10h	10.0	DPT4_10h_T40	22.73	16.62	0.88	FE
	12h	12.0	DPT5_12h_T40	25.02	18.29	0.78	D
	24h	24.0	DPT6_24h_T40	24.94	18.23	0.58	D+SE+CC
		25.0	DPT7_24h_T40	24.82	18.14	0.62	D
	72h	72.2	DPT8_72h_T40	27.91	20.40	0.56	D+CC
		73.3	DPT9_72h_T40	27.57	20.15	0.73	D
	7d	168.3	DPT10_7d_T40	27.97	20.45	0.72	D

2 Notes: FE=cohesive shear failure in epoxy; D=debonding at CFRP-epoxy interface; CC=concrete cracking;

3 SE=splitting of epoxy.

4

1 Table 4 – Regression parameters obtained from model for the evolution of pull-out force

T_{cure}	F_{ult} [kN]	λ	β	R^2
20 °C	25.45	14.275	3.374	0.982
30 °C	27.76	9.585	3.058	0.972
40 °C	27.82	7.312	3.012	0.969

2

1 Table 5 – Kinetic parameters obtained from autocatalytic isothermal model

Denomination	**m**	**n**	**k**	**R^2**	**E_a [kJ/mol]**	**A [min^{-1}]**
EMM1_T20	0.672	1.873	11.455	0.839		
EMM2_T20	0.658	1.799	11.848	0.936	↑	↑
EMM1_T30	0.864	2.072	25.729	0.971	34.55	57192529545
EMM2_T30	0.837	1.969	25.316	0.975	↓	↓
EMM1_T40	0.875	1.986	25.969	0.963		

2

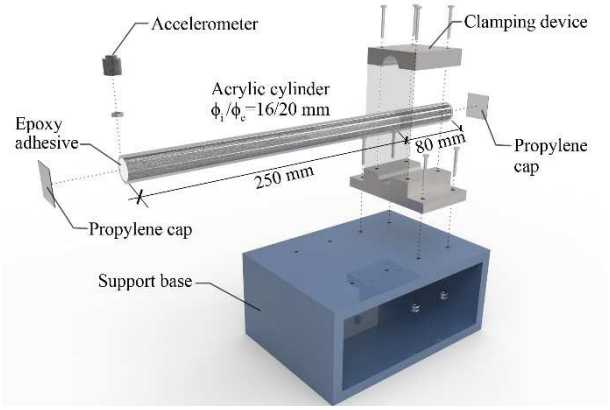

Figure 1 – Experimental setup of EMM-ARM tests (exploded view).

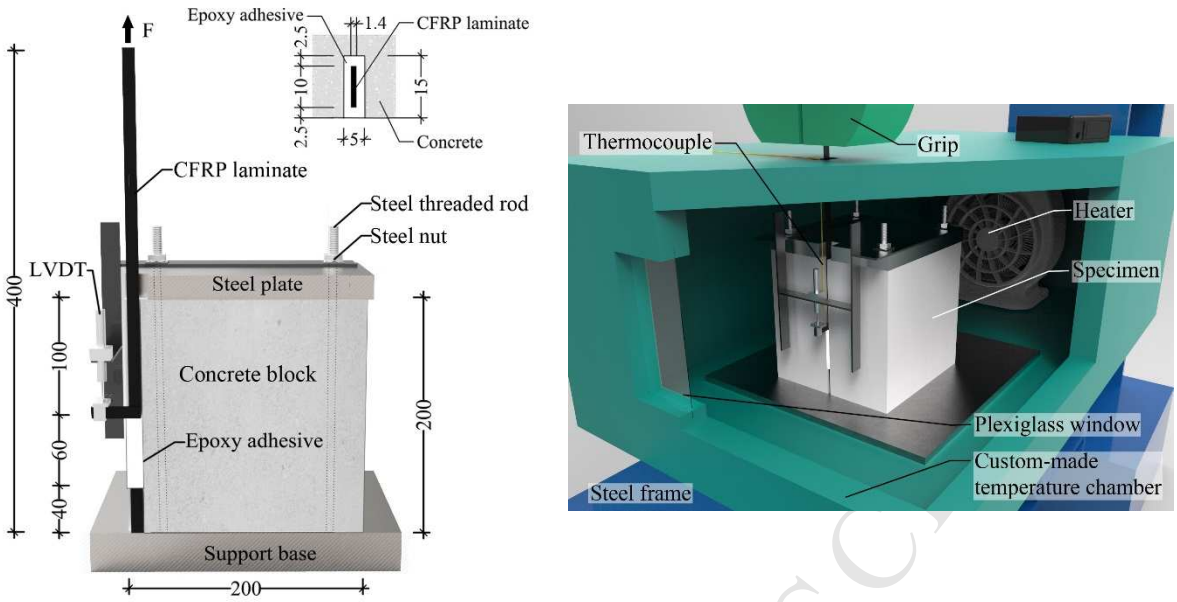

(a) (b)

Figure 2 – Configuration of direct pull-out tests: (a) cross-section of the specimen; (b) view of the experimental setup.

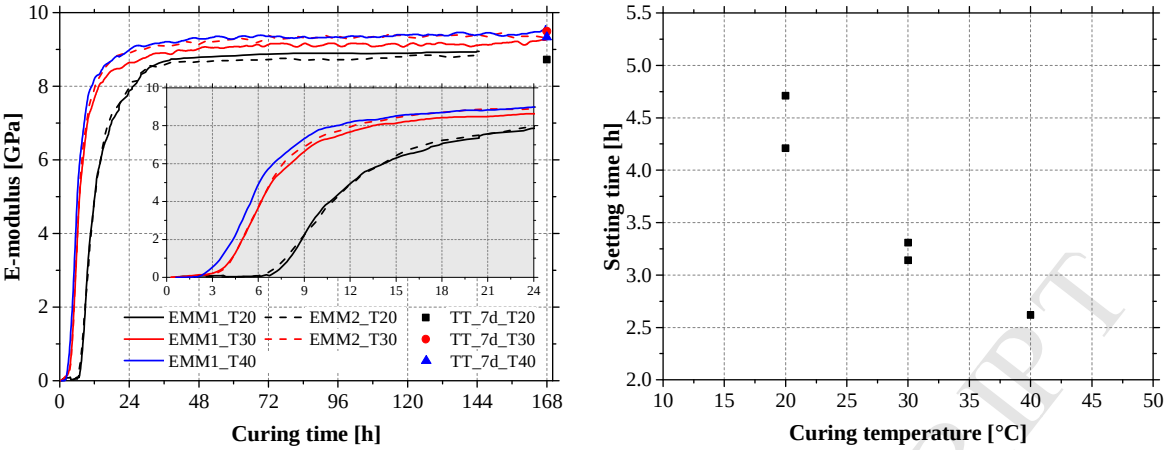

(a) (b)

Figure 3 – (a) Evolution of epoxy E-modulus along curing time; (b) setting time *versus* curing temperature.

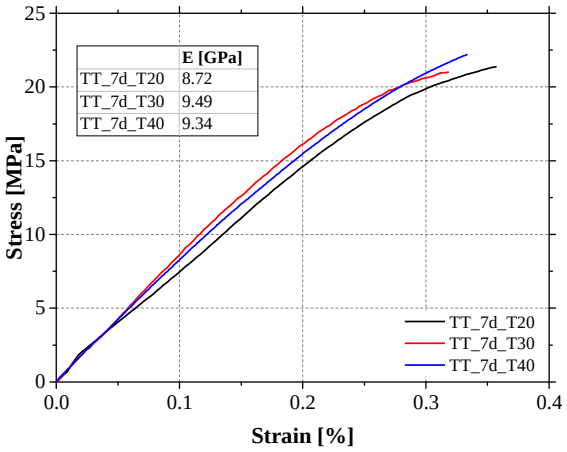

1

2 Figure 4 – Average stress-strain curves obtained by tensile tests

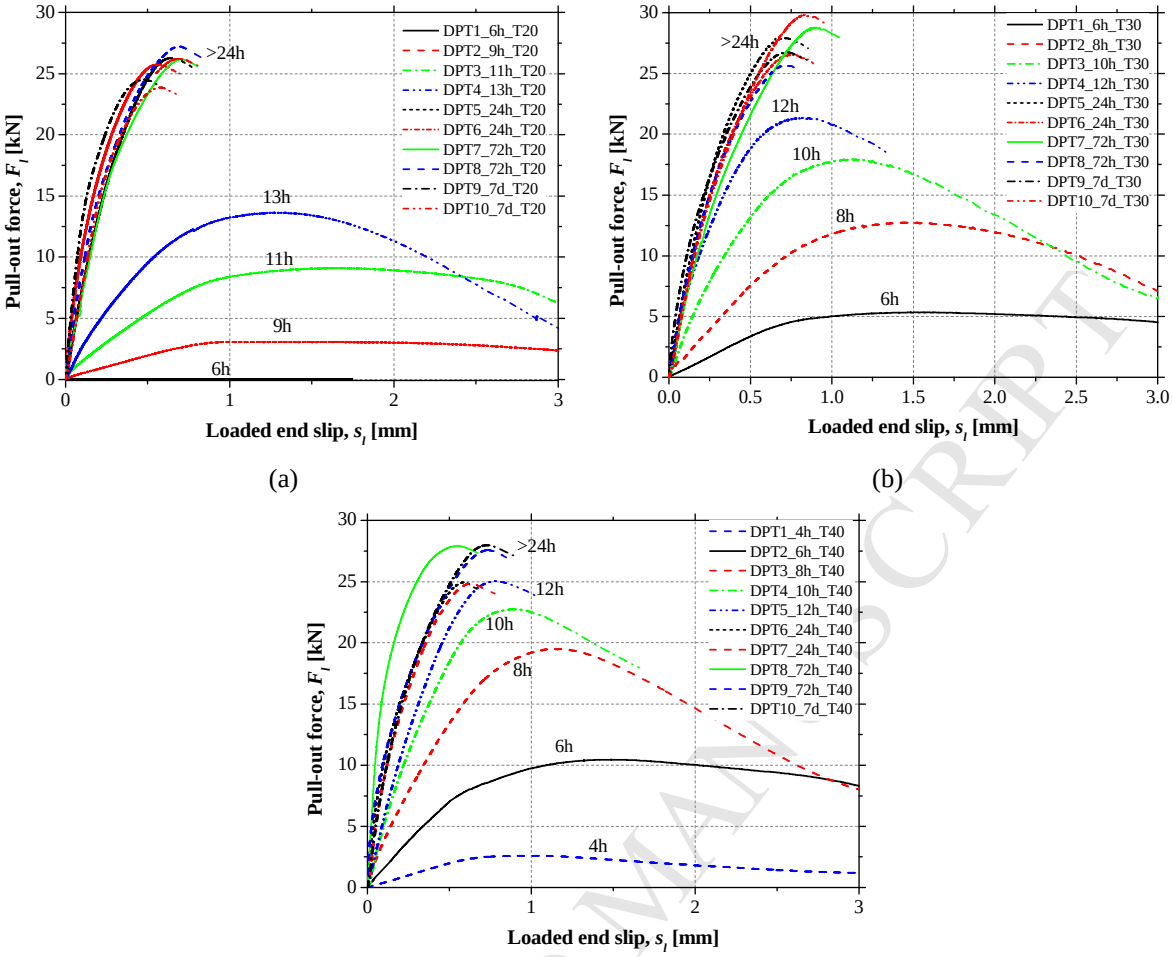

1 Figure 5 – Pull-out force *versus* loaded end slip during curing time at different temperatures: (a)

2 20 °C; (b) 30 °C and (c) 40 °C.

3

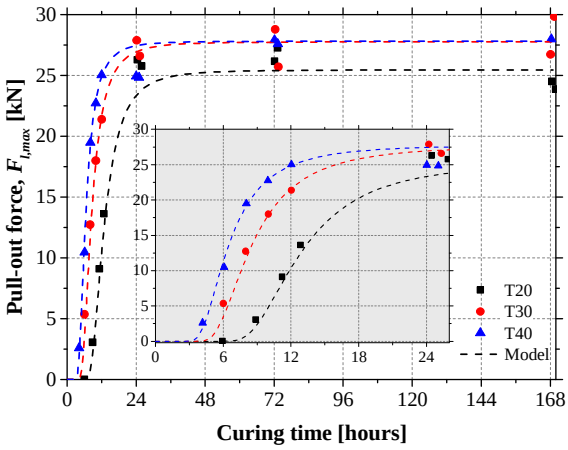

Figure 6 – Pull-out force *versus* curing time at different temperatures.

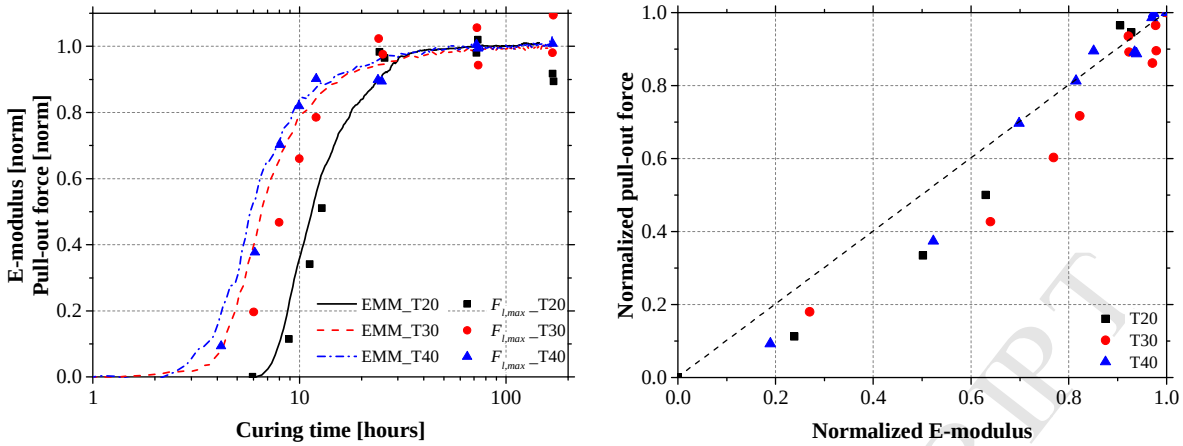

(a) (b)

Figure 7 – (a) Epoxy E-modulus and peak pull-out force along curing time, normalized to 72 hours; (b) Relationship between epoxy E-modulus and pull-out force.

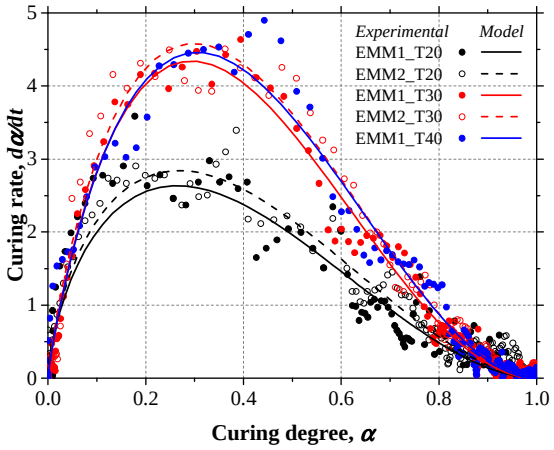

Figure 8 - Curing rate *versus* curing degree: comparison of experimental and autocatalytic model results.

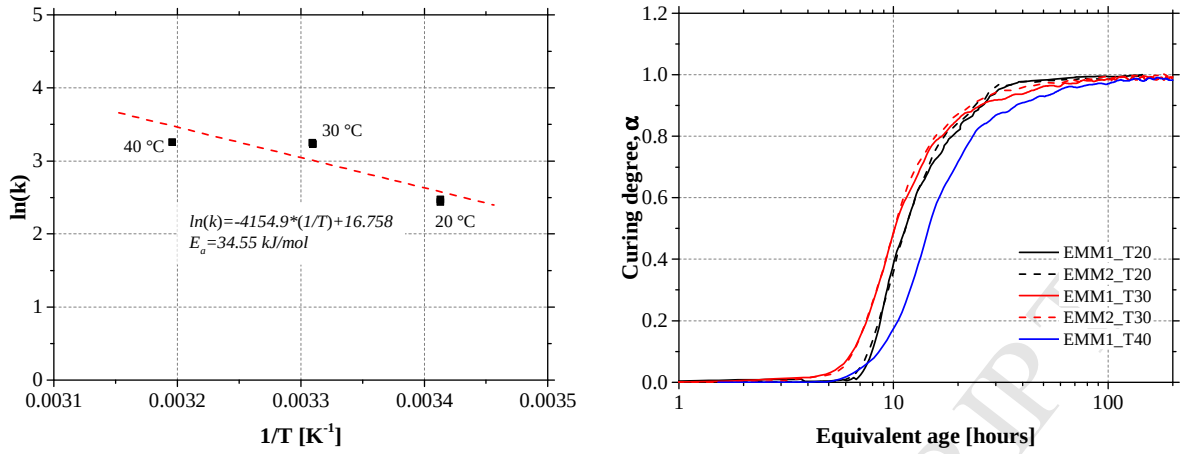

(a) (b)

1 Figure 9 - Autocatalytic model: (a) Arrhenius plot of rate coefficient; (b) Curing degree of epoxy

2 adhesive *versus* equivalent age.

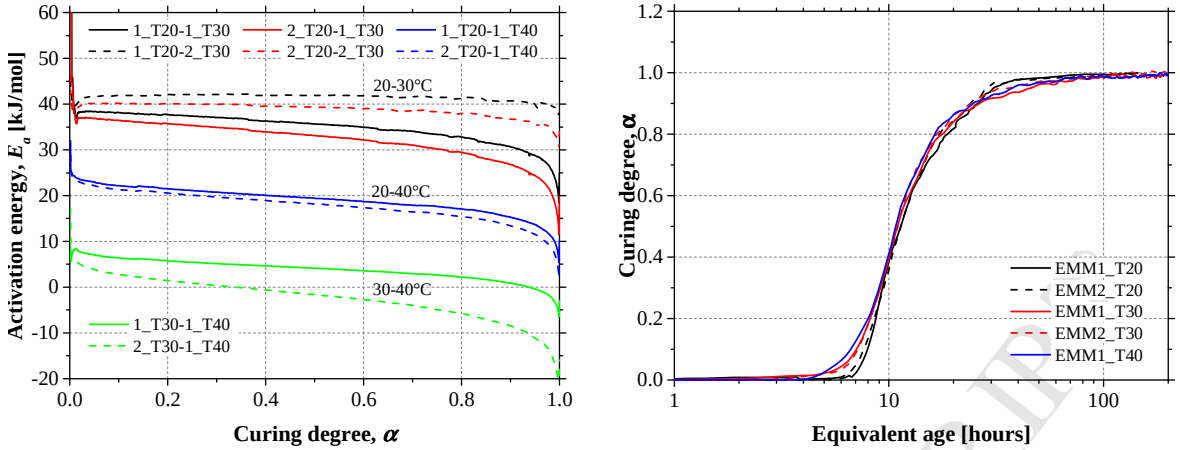

(a) (b)

1 Figure 10 – Model-free method applied to epoxy E-modulus: (a) Activation energy *versus* curing
2 degree; (b) normalized E-modulus of epoxy adhesive *versus* equivalent age (reference: 20 °C).

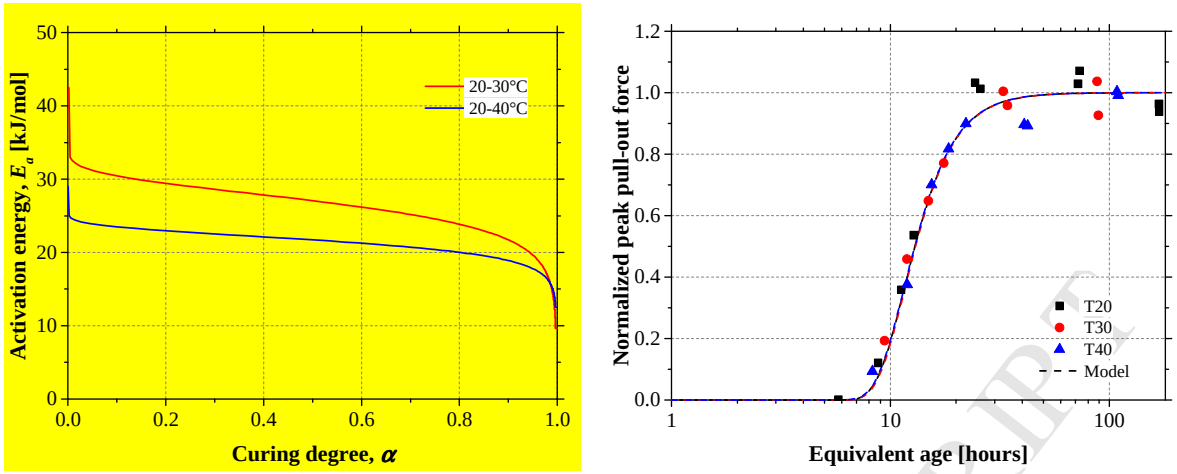

(a) (b)

1 Figure 11 – Model-free method applied to pull-out force: (a) Activation energy *versus* curing degree

2 for the pull-out force; (b) Pull-out force *versus* equivalent age (reference: 20 °C).

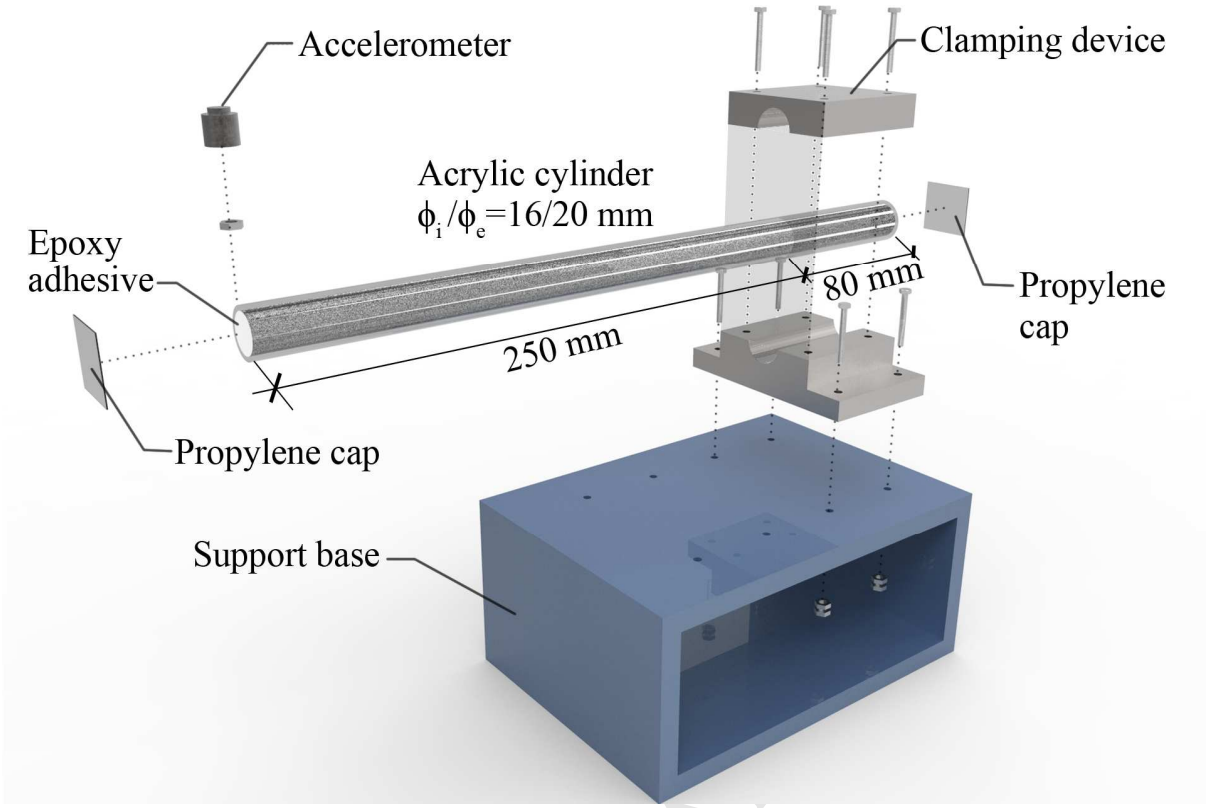

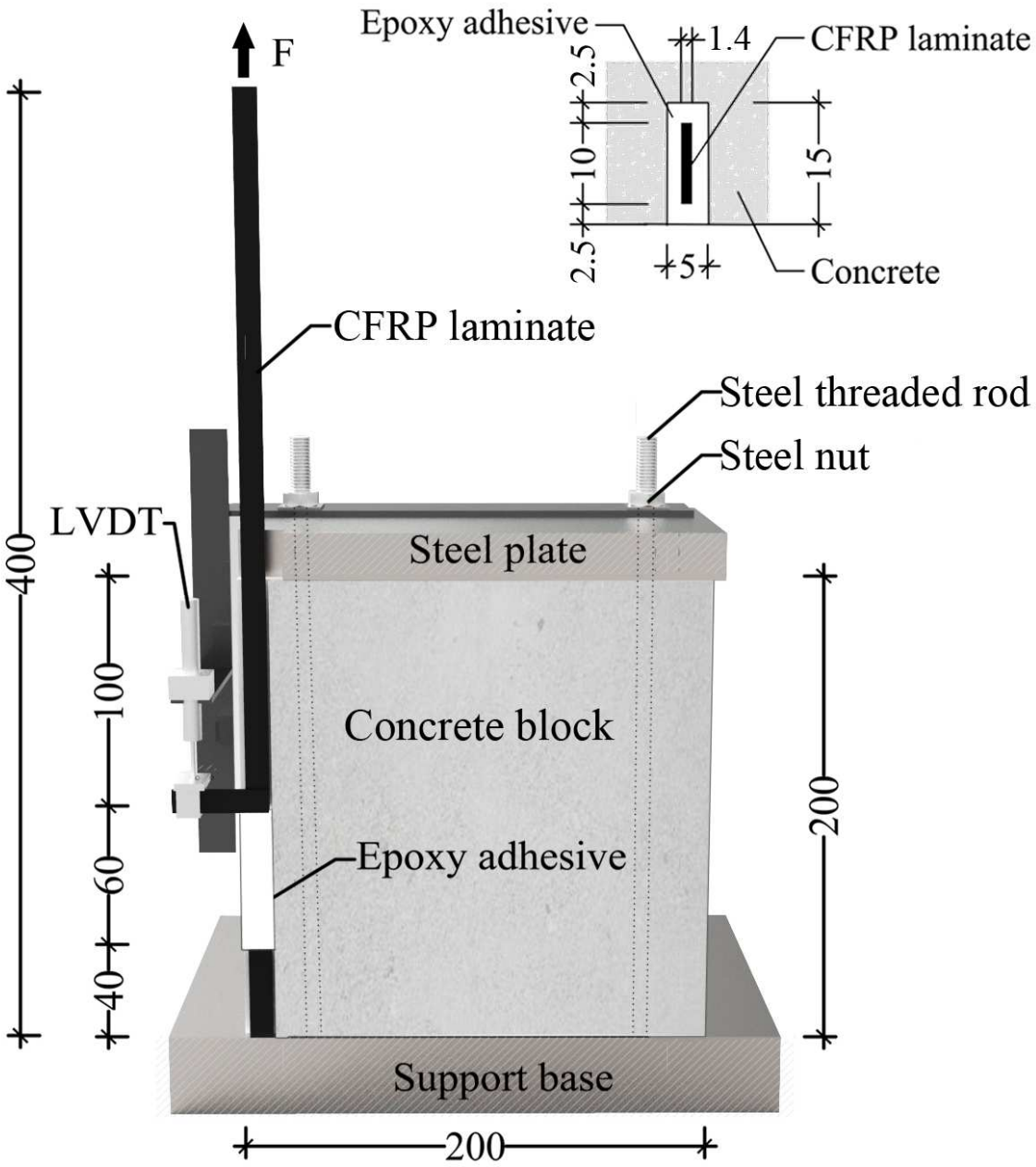
Epoxy adhesive
1.4
CFRP laminate
2.5
10
15
2.5
5
Concrete
F
CFRP laminate
Steel threaded rod
Steel nut
LVDT
Steel plate
400
100
60
40
Concrete block
200
Epoxy adhesive
Support base
200

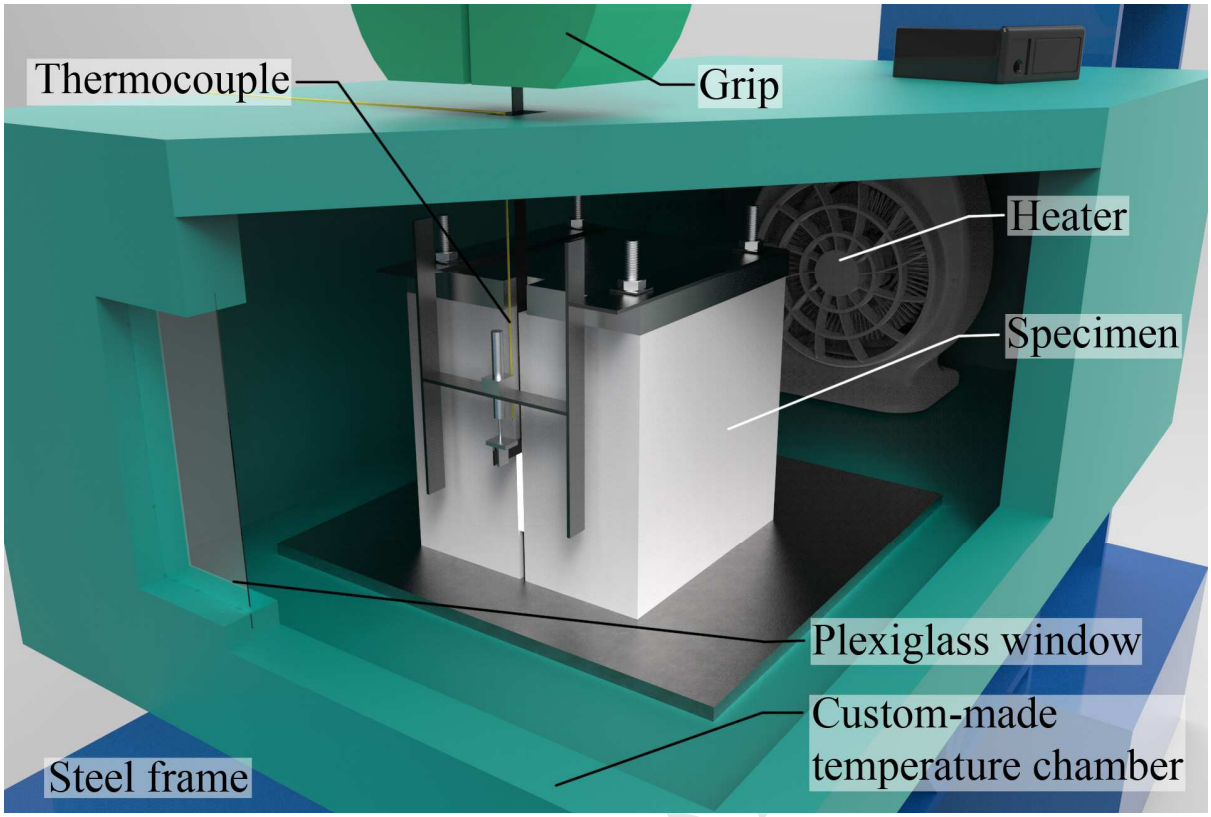

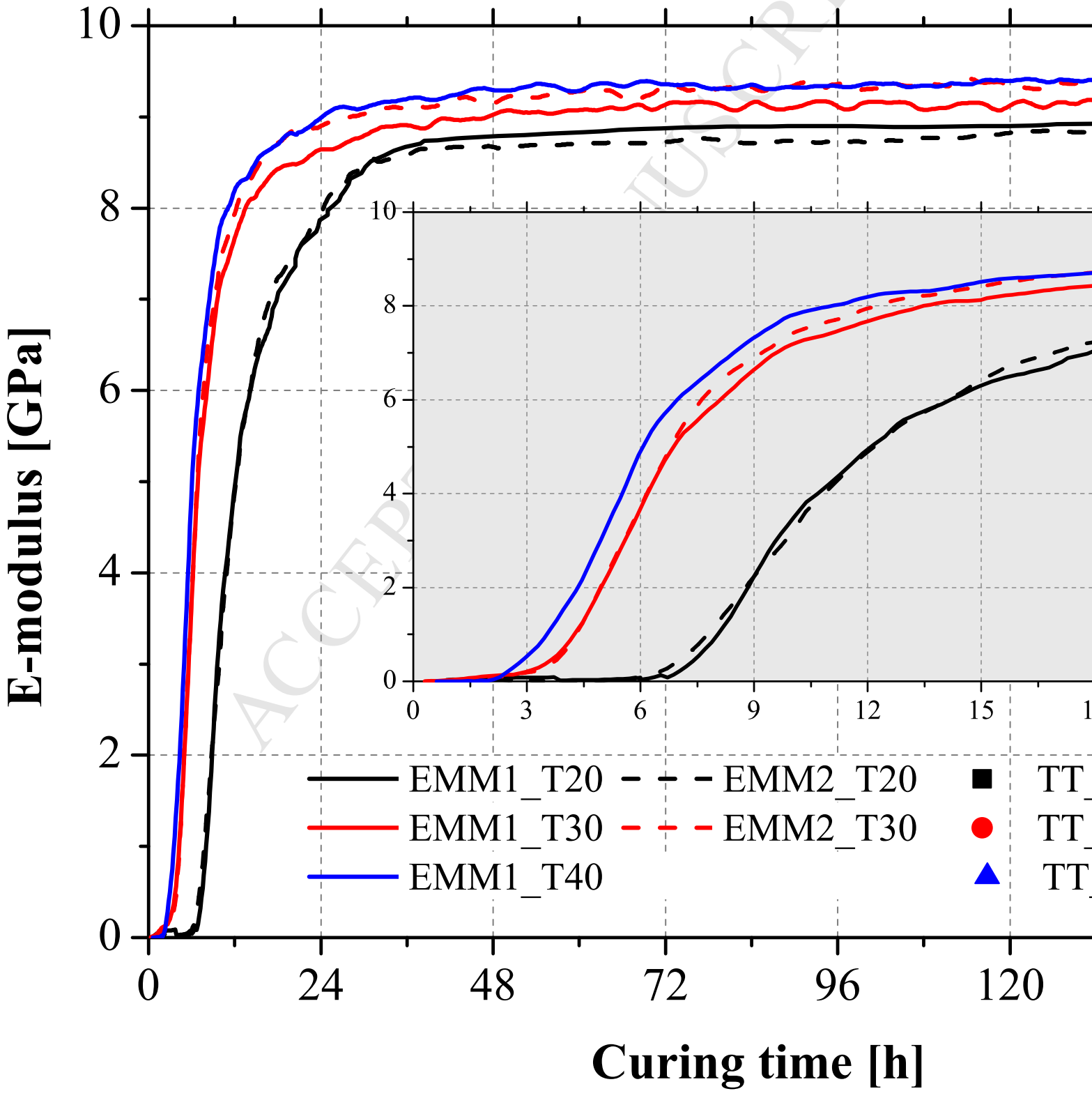
E-modulus [GPa]
Curing time [h]
0
2
4
6
8
10
0
24
48
72
96
120
0
3
6
9
12
15
EMM1_T20
EMM2_T20
EMM1_T30
EMM2_T30
EMM1_T40
TT_
TT_
TT_